

Multiple Inverters Operated in Parallel for Proportional Load Sharing in Microgrid

Chethan Raj D¹, D N Gaonkar²

Department of Electrical and Electronics Engineering, National Institute of Technology Karnataka, Surathkal, India

Article Info

Article history:

Received Jan 30, 2017

Revised Mar 30, 2017

Accepted Apr 14, 2017

Keyword:

Distributed generation

Droop control

Microgrid

Parallel inverter

Three phase inverter

ABSTRACT

The new energy source utilization and development, gradual rise of distributed power grid miniaturization, intelligence, control has become a trend. In order to make microgrid reliable and efficiently run, control technology of microgrid has become a top priority and an inverter as microgrid basic unit, its control has become the most important part in microgrid. In this paper, three inverters are operated in parallel using an P-V/Q-F droop control is investigated. Mathematical model of three phase inverter with LC filter is derived, which is based on the voltage and current dual control loop. Parallel control strategy based on P-V/Q-F droop control, does not require a real time communications between the inverters and more suitable for microgrid applications. To verify the feasibility and validity of the droop control scheme, simulation is done in Matlab/Simulink and results indicate droop control has significant effect on power sharing and balancing the voltage magnitude, frequency.

Copyright © 2017 Institute of Advanced Engineering and Science.
All rights reserved.

Corresponding Author:

Chethan Raj D,
Department of Electrical and Electronics Engineering,
National Institute of Technology Karnataka,
Surathkal, Mangalore, Karanataka, India.
Email: chethanraj9@gmail.com

1. INTRODUCTION

With including wind power, solar and other renewable energy sources and clean and efficient fossil fuel power generation, including the development of new technologies, distributed generation system are becoming popular to meet the load growth [1]-[2]. An effective way to take advantage of the efficiency and reliability of power supply. DGS with less investment, flexible power generation, can be compatible with the environment, and it is widely used in the power system network, but large-scale penetration DGS also has some negative impacts, such as distributed generation stand-alone high access costs, control is more complex [3]. In addition, from the perspective of the system to analyze, DGS is not controllable power generating unit, so the system is always trying to take the isolated operation. According to the literature [4], when the power system fails, DGS must immediately out of operation, but this limits the operating mode of distributed generation, weakening its advantages and potential. To integrate the advantages of distributed generation and to reduce negative impact of distributed generation on the grid, to optimize the efficiency and value of DGS, relevant experts proposed the concept of micro-grid [5-6,21]. DGs are connected to load through inverter interface in microgrid. Currently, the AC electrical load and power quality requirements are high, by increasing the single inverter capacity will lead to more load on the inverter and electrical dependent increases [7]. The inverters in parallel can achieve high power, reliable and redundant power [8]. There are many ways to achieve parallel control of inverter in microgrid. Master slave control [9], active current distribution control [10], droop control [11]-[13]. Master slave control strategy needs to focus all inverters power supply information and send it to control centre. Therefore, this strategy requires a corresponding communication line to transmit acquisition and control information [9]. active current distribution control is

provided with a reference current for each inverter in parallel, the drawback is single inverter failure will cause the entire parallel system failure [10]. Droop control avoids the adverse effects of the communication failure of the inverter. Advantages of droop control is that no contact between the inverters signal line, thus reducing the unreliability of the system, the cost is relatively low, you can plug and play, allowing the system to achieve true redundancy [14]-[16]. In this paper, P-V/Q-F droop control is implemented for parallel inverters in microgrid using Matlab/Simulink simulation environment, to verify the effectiveness of the model design and control.

2. MICROGRID DROOP CONTROL PRINCIPLE

Consider an ac bus connected to an inverter equivalent circuit is shown in Figure 1. Inverter output voltage is $E\angle\delta$, the common load terminal voltage is $V\angle 0$, the output of the inverter and a common load end through the inverter connected to the output impedance. The total inverter output impedance is set as $Z\angle\theta$, which itself includes an inverter output impedance $Z_b\angle\theta_b$ and the line impedance is $Z_L\angle\theta_L$.

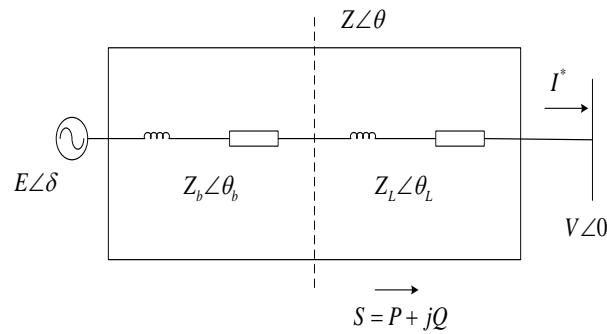


Figure 1. AC bus inverter equivalent circuit schematic

The DG unit output power is:

$$P + jQ = \bar{S} = V \bar{I}^* = V \left(\frac{Ee^{j\delta} - V}{Ze^{j\theta}} \right)^* \quad (1)$$

Output current is:

$$\bar{I} = \frac{Ee^{j(\delta-\theta)} - Ve^{-j\theta}}{Z} = \frac{E \cos(\delta-\theta) - V \cos \theta}{Z} + j \frac{E \sin(\delta-\theta) + V \sin \theta}{Z} \quad (2)$$

(2) into Equation (1) to give the dg unit output of active and reactive power are as follows:

$$P = \frac{V}{Z} [E \cos(\delta-\theta) - V \cos \theta] \quad (3)$$

$$Q = -\frac{V}{Z} [E \sin(\delta-\theta) + V \sin \theta] \quad (4)$$

(3) and (4) through simplification can be written as:

$$P = \frac{V}{Z} [(E \cos \delta - V) \cos \theta + E \sin \delta \sin \theta] \quad (5)$$

$$Q = \frac{V}{Z} [(E \cos \delta - V) \sin \theta - E \sin \delta \cos \theta] \quad (6)$$

Inverter output impedance is $Z e^{j\theta} = R + jX$ is substituted into the equation (5) and (6) to give:

$$P = \frac{V}{R^2 + X^2} [R(E \cos \delta - V) + XE \sin \delta] \quad (7)$$

$$Q = \frac{V}{R^2 + X^2} [X(E \cos \delta - V) - RE \sin \delta]$$

According to the Equation (7), the transfer impedance is inductive $\theta = 90^\circ$, so active and reactive equation is given by:

$$P = \frac{EV \sin \delta}{X} \quad (8)$$

$$Q = \frac{EV \cos \delta - V^2}{X} \quad (9)$$

Typically connection impedance is much smaller than the load impedance, δ is very small, thus $\sin \delta = \delta, \cos \delta = 1$ substituted into the equation (8) and (9) to give:

$$P = \frac{EV \delta}{X} \quad (10)$$

$$Q = \frac{EV - V^2}{X} \quad (11)$$

As it can be seen from the Equation (10) and (11), active and power-related angle, which is related to the frequency of the output voltage, reactive power and voltage amplitude related to the difference, it is possible to use active power to adjust the frequency, reactive power to regulate the voltage amplitude, which is the traditional droop control [10]-[11]. The droop control equation is given by

$$\omega = \omega^* - m(P - P^*) \quad (12)$$

$$E = E^* - n(Q - Q^*) \quad (13)$$

The inverter no-load output voltage amplitude and frequency are V^*, ω^* , active and reactive droop co-efficients are m, n. The inverter rated output active and reactive power are P^*, Q^* . When the transfer impedance is purely resistive that $\theta = 0$, the same above derivation of active and reactive power can be obtained:

$$P = \frac{EV - V^2}{R} \quad (14)$$

$$Q = \frac{EV \delta}{R} \quad (15)$$

By Equation (14) and (15) can be seen, the difference between active and voltage amplitude related to reactive power and power related angle, which is P-V/Q-F droop control method. m, n droop co-efficients.

$$\omega = \omega^* + n(Q - Q^*) \quad (16)$$

$$E = E^* - m(P - P^*) \quad (17)$$

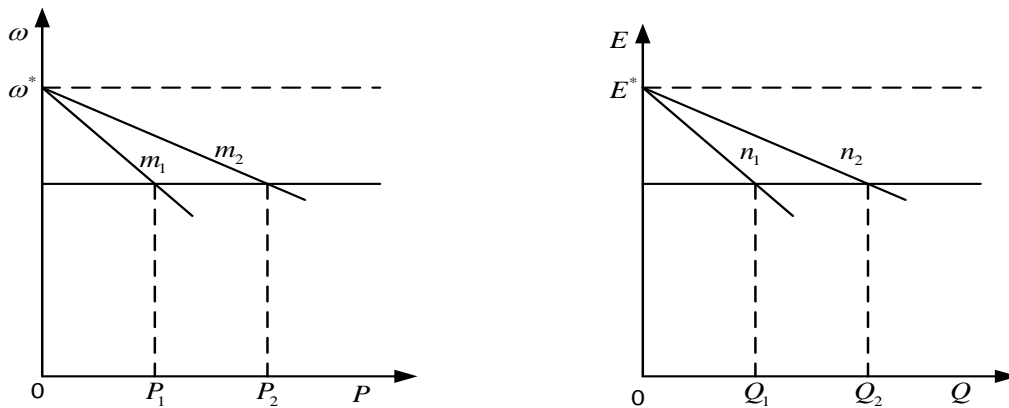


Figure 2. Droop Control Curve

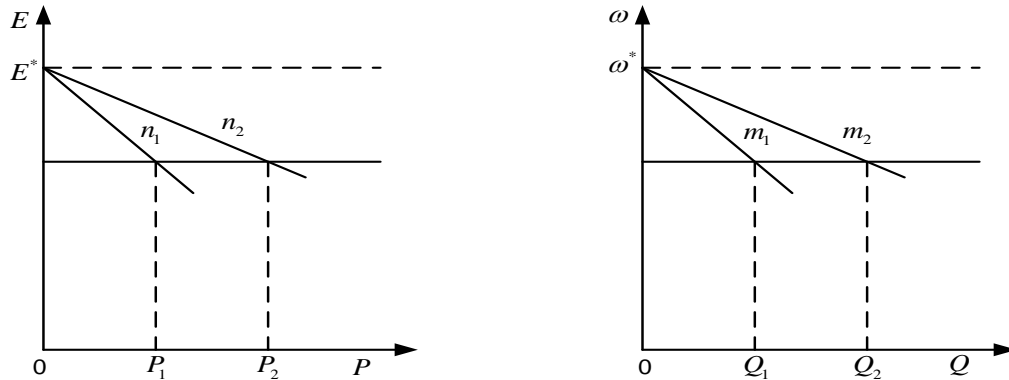


Figure 3. Reverse Droop Control Curve

3. MODELING OF MICROGRID

3.1. Microgrid Block Diagram

Microgrid is mostly a miniature power, namely small units contain power electronics interface, including microturbines, fuel cells, photovoltaic cells, batteries and other storage unit. Microgrid as a whole is composed of a voltage source inverters using SPWM modulation as shown in the Figure 4, then assuming that the inverter dc bus voltage V_{dc} essentially unchanged L_{f1}, L_{f2}, L_{f3} is a three phase filter inductor, r_1, r_2, r_3 filter inductor equivalent resistance, C_{f1}, C_{f2}, C_{f3} is a three phase filter capacitor. Comprehensive equivalent line impedance of the transmission line of three inverters is expressed as $Z_1=R_1+jX_1, Z_2=R_2+jX_2, Z_3=R_3+jX_3$, PCC represents a common connection point for inverters.

3.2. Three Phase Inverter dq model

Three phase voltage source inverter with three phase full bridge topology the details of the structure as shown in the Figure 5. Inverter leg midpoint voltage V_A, V_B, V_C . Inverter output terminal voltage v_{ao}, v_{bo}, v_{co} . Three phase inductor current respectively i_{La}, i_{Lb}, i_{Lc} . Load side three phase inverter output current [17]-[18]. According to Kirchhoff's voltage law and current law can be obtained as:

$$V_A - v_{ao} = L_f \frac{di_{La}}{dt} + r_{La}, V_B - v_{bo} = L_f \frac{di_{Lb}}{dt} + r_{Lb}, V_C - v_{co} = L_f \frac{di_{Lc}}{dt} + r_{Lc} \quad (18)$$

Kirchhoff's current law can be obtained as:

$$i_{La} - i_{ao} = C_f \frac{dv_{ao}}{dt}, i_{Lb} - i_{bo} = C_f \frac{dv_{bo}}{dt}, i_{Lc} - i_{co} = C_f \frac{dv_{co}}{dt} \quad (19)$$

According to the principle of equal amplitude conversion, its transformation matrix is:

$$T_{abc-\alpha\beta} = \frac{2}{3} \begin{bmatrix} 1 & -\frac{1}{2} & -\frac{1}{2} \\ 0 & \frac{\sqrt{3}}{2} & -\frac{\sqrt{3}}{2} \end{bmatrix} \quad (20)$$

three phase voltage source inverter $\alpha\beta$ equation of state two phase stationary co-ordinate system:

$$\frac{d}{dt} \begin{bmatrix} i_{L\alpha} \\ i_{L\beta} \\ v_{o\alpha} \\ v_{o\beta} \end{bmatrix} = \begin{bmatrix} -\frac{r}{L_f} & 0 & -\frac{1}{L_f} & 0 \\ 0 & -\frac{r}{L_f} & 0 & -\frac{1}{L_f} \\ \frac{1}{C_f} & 0 & 0 & 0 \\ 0 & \frac{1}{C_f} & 0 & 0 \end{bmatrix} \begin{bmatrix} i_{L\alpha} \\ i_{L\beta} \\ v_{o\alpha} \\ v_{o\beta} \end{bmatrix} + \begin{bmatrix} 0 & 0 & \frac{1}{L_f} & 0 \\ 0 & 0 & 0 & \frac{1}{L_f} \\ -\frac{1}{C_f} & 0 & 0 & 0 \\ 0 & -\frac{1}{C_f} & 0 & 0 \end{bmatrix} \begin{bmatrix} i_{o\alpha} \\ i_{o\beta} \\ v_{\alpha} \\ v_{\beta} \end{bmatrix} \quad (21)$$

According to the principle of equal amplitude transformation, $\alpha\beta$ two phase rotating co-ordinate transformation matrix is:

$$T_{\alpha\beta-dq} = \begin{bmatrix} \cos(\omega t) & \sin(\omega t) \\ -\sin(\omega t) & \cos(\omega t) \end{bmatrix} \quad (22)$$

$$\frac{d}{dt} \begin{bmatrix} v_{od} \\ v_{oq} \\ i_{Ld} \\ i_{Lq} \end{bmatrix} = \begin{bmatrix} 0 & \omega & \frac{1}{C_f} & 0 \\ -\omega & 0 & 0 & \frac{1}{C_f} \\ -\frac{1}{L_f} & 0 & -\frac{r}{L_f} & \omega \\ 0 & -\frac{1}{L_f} & -\omega & -\frac{r}{L_f} \end{bmatrix} \begin{bmatrix} v_{od} \\ v_{oq} \\ i_{Ld} \\ i_{Lq} \end{bmatrix} + \begin{bmatrix} -\frac{1}{C_f} i_{od} \\ -\frac{1}{C_f} i_{oq} \\ \frac{v_d}{L_f} \\ \frac{v_q}{L_f} \end{bmatrix} \quad (23)$$

Equation (23) is the three phase voltage source inverter dq mathematical model in two phase rotating co-ordinate system.

3.3. Voltage and current dual loop

The typical voltage and current dual loop control strategy, which has fast response, can automatically and easily achieve both limiting flow in parallel inverter. Its control structure as shown in the Figure 6. The output voltage is compared with a reference voltage signal and the resulting error signal through the instantaneous voltage as current inner loop PI controller setpoint reference. Inverter bridge output filter inductor current and the current given reference signal is compared, the error signal obtained through instantaneous current loop PI controller as SPWM modulated voltage signal [19]. The introduction of the inner filter inductor current improves the stability of the microgrid system. The design of voltage loop and current loop are given in the following section.

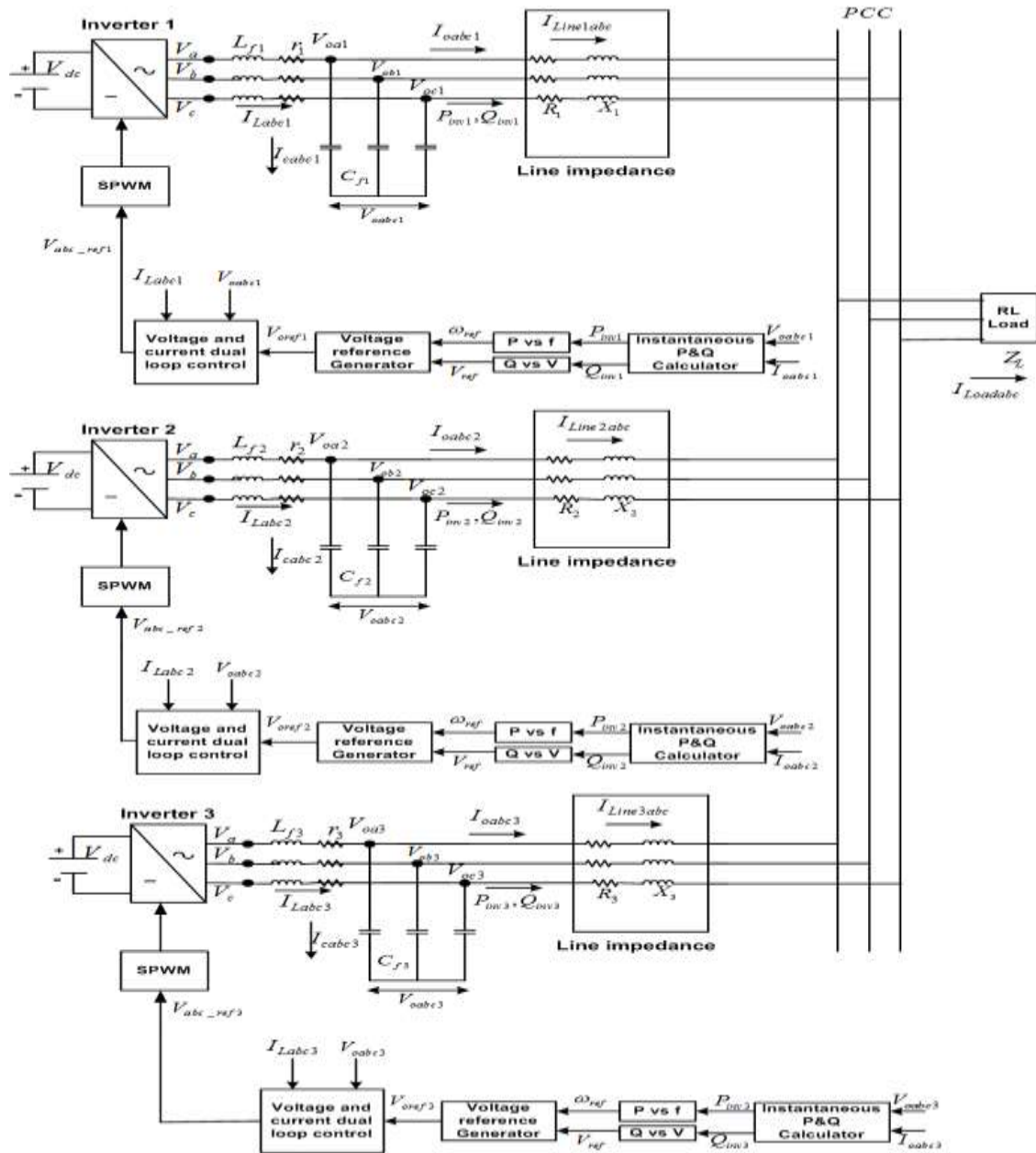


Figure 4. Droop control block diagram of parallel inverter

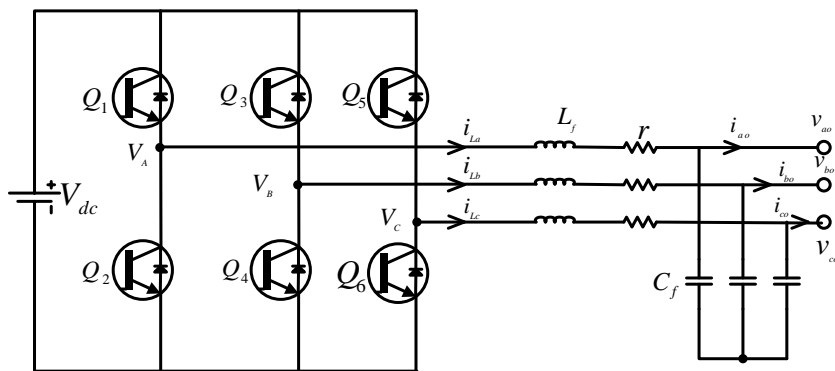


Figure 5. Three phase voltage source inverter topology

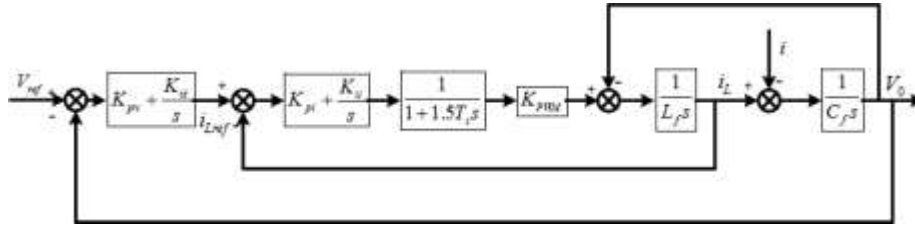


Figure 6. Voltage and current double closed loop control block diagram

3.4. Current Loop

Where, T_s is a current loop sampling period, K_{ip} and K_{ii} PI controller parameters corresponding to the current loop, $1/(1+0.5T_s s)$ on behalf of inertia pwm control, $1/(1+T_s s)$ for the current sampling delay and K_{pwm} represents the equivalent gain of the inverter ($K_{pwm} = V_{dc}/2$). take the inner current loop cut off frequency

$$f_{ib} = \frac{1}{5} f_s = 2000Hz.$$

the open loop transfer function given by:

$$G_{oi} = \frac{K_{PWM} K_{ii} (1 + \frac{K_{ip}}{K_{ii}} s)}{rs(1 + 1.5T_s r)(1 + \frac{L_f}{r} s)} \tag{24}$$

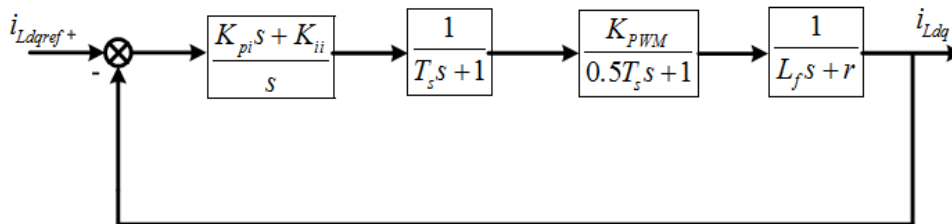


Figure 7. Block diagram of the current loop

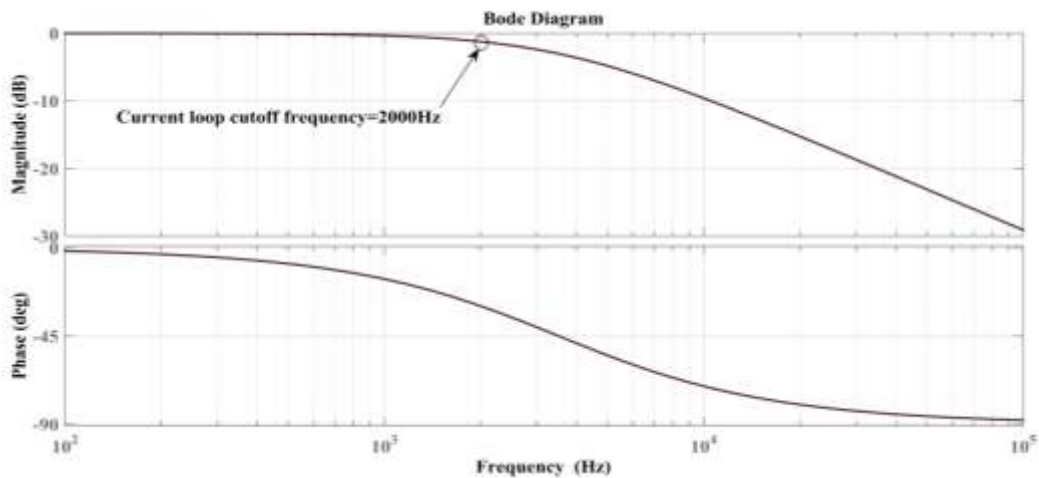


Figure 8. Bode diagram of the current loop

The closed loop transfer function of the current loop is:

$$G_{ci} = \frac{G_{oi}(s)}{1+G_{oi}(s)} = \frac{\frac{K_{PWM}K_{ii}}{1.5T_s r}}{s^2 + \frac{1}{1.5T_s}s + \frac{K_{PWM}K_{ii}}{1.5T_s r}} \quad (25)$$

$$G_{ci} = \frac{\omega_n^2}{s^2 + 2\xi\omega_n s + \omega_n^2}, \xi = \frac{1}{2} \sqrt{\frac{r}{1.5K_{PWM}K_{ii}T_s}} = 0.707, \omega_n = \sqrt{\frac{K_{PWM}K_{ii}}{1.5T_s r}} \quad (26)$$

$$K_{ii} = \frac{r}{3T_s K_{PWM}}, K_{ip} = \frac{L_f}{3T_s K_{PWM}}, K_{ii} = 1.90, K_{pi} = 0.02857 \quad (27)$$

3.5. Voltage Loop

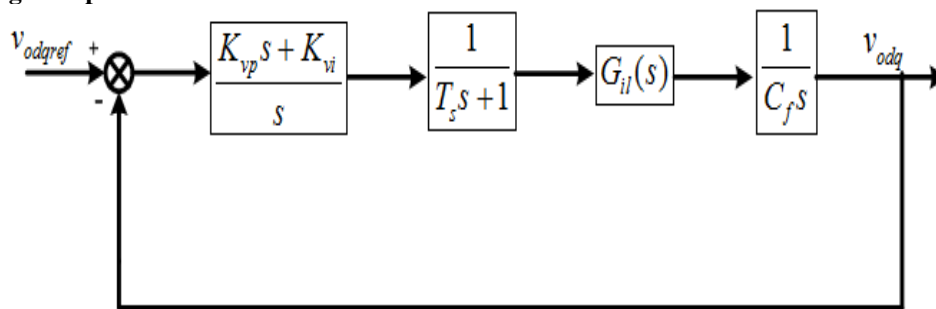


Figure 9. Block diagram of the voltage loop

When type1 system designed according to the typical current loop, it can be approximately equivalent to inertia time constant of $3T_s$.

$$G_{ci} = \frac{1}{1+3T_s s} \quad (28)$$

The cut-off frequency of the voltage loop should be less than 1/2 of the current loop, voltage loop selection cut off frequency of 800Hz.

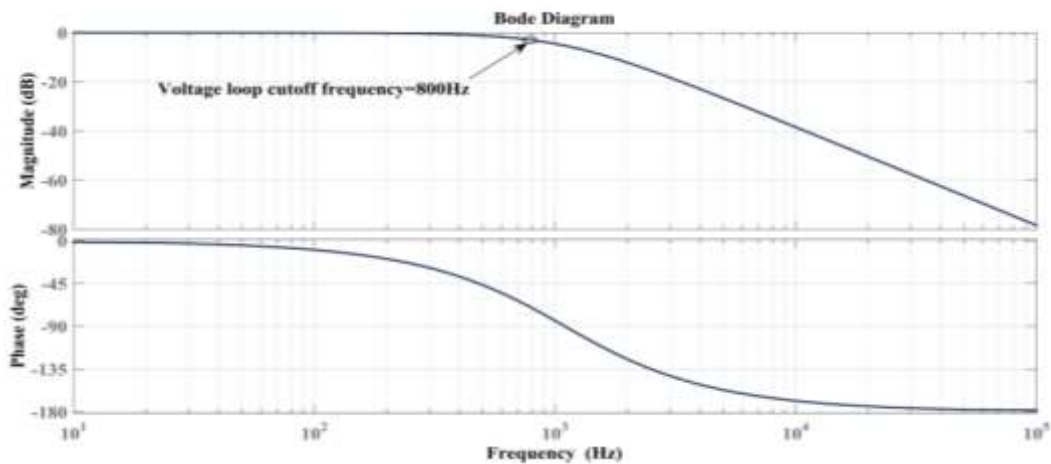


Figure 10. Bode diagram of the voltage loop

To ensure the micro grid inverter parallel operation can maintain a constant voltage in microgrid system. accordance with its typical type 2 systems design, the voltage loop bandwidth is given by:

$$h_u = \frac{K_{vp}}{4T_s K_{vi}} \quad (29)$$

type 2 system parameters based on typical tuning relations have:

$$\frac{K_{vi}}{C} = \frac{h_u + 1}{32h_u^2 T_s^2} \quad (30)$$

Take the bandwidth $h_u=2$ into (30) can be obtained as:

$$K_{vi} = \frac{1.5C}{64T_s^2} = 35.15 \quad (31)$$

$$K_{vp} = \frac{1.5C}{10T_s} = 0.0225 \quad (32)$$

Table 1. Parameters for inverter parallel operation

Parameters	Inverter 1	Inverter 2	Inverter 3
Rating	3KVA	3KVA	3KVA
DC link voltage(V_{dc})	700V	700V	700V
Switching			
Frequency(f_s)	10KHz	10KHz	10KHz
Fundamental			
Frequency(f_n)	50Hz	50Hz	50Hz
Nominal			
Voltage(V_o)	311V	311V	311V

3.6. Simulation Results

In this section, the P-V/Q-F droop control for parallel inverters is investigated using Matlab/Simulink simulation platform. Microgrid system consists of three inverter interface as shown in the Figure 4 and control parameters are given in the Table 1. The following two cases are discussed in the following section.

3.6.1. Case 1: Power sharing of inverters in microgrid with constant power load

Three inverters are connected in parallel and droop co-efficients and line impedance are taken as $m_1=m_2=m_3=0.0015V/VAR$, $n_1=n_2=n_3=00001rad/s/W$ and $R_1=R_2=R_3=0.642\Omega$, $X_1=X_2=X_3=0.0264\Omega$. Power sharing of each individual inverters with load $P_{Load}=4500W, Q_{Load}=10VAR$ and each inverters is able to share the load proportionally, active power of $P_1=1495W, P_2=1492W, P_3=1488W$ as shown in the Figure 11 and reactive power of $Q_1=2.6VAR, Q_2=2.4VAR, Q_3=2.1VAR$ as shown in the Figure12. Frequency variation is within the range of 49.99Hz to 49.98Hz, the maximum fluctuation of 0.004Hz as shown in the Figure 13. Voltage at PCC can be seen as a slight decline in the voltage amplitude by a 311V to 310V as shown in the Figure 14. Thus, P-V/Q-F droop control ensures that the voltage change is not greater than 5%, the frequency change is not greater than 1% and established a better accuracy and effectiveness in the microgrid system.

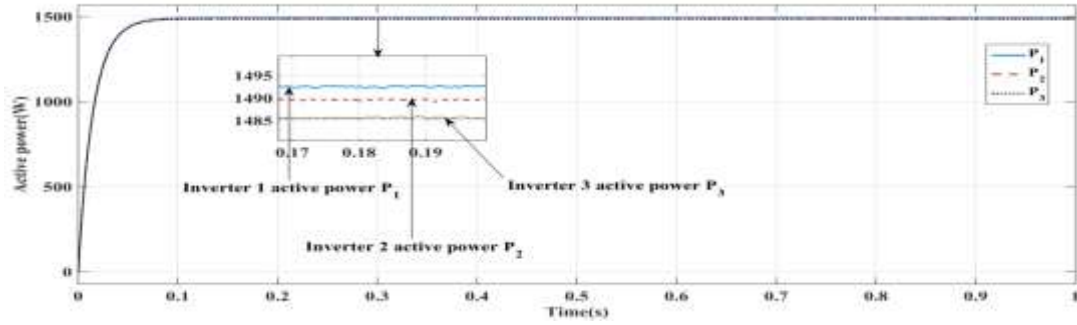


Figure 11. Active power waveforms of inverters with constant power load

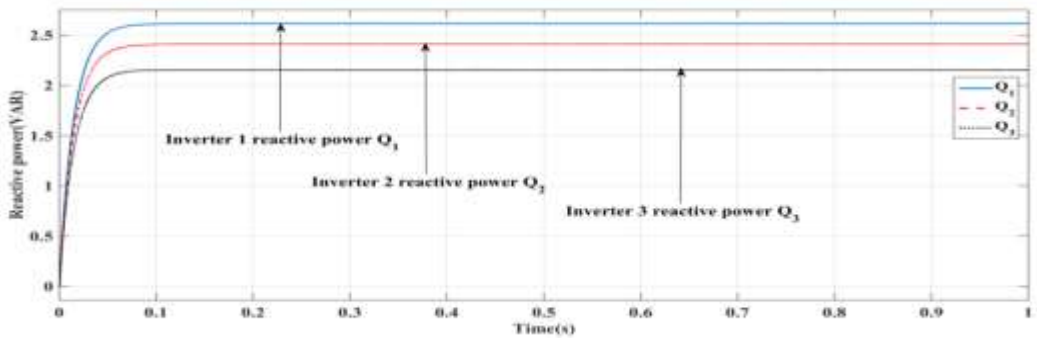


Figure 12. Reactive power waveforms of inverters with constant load

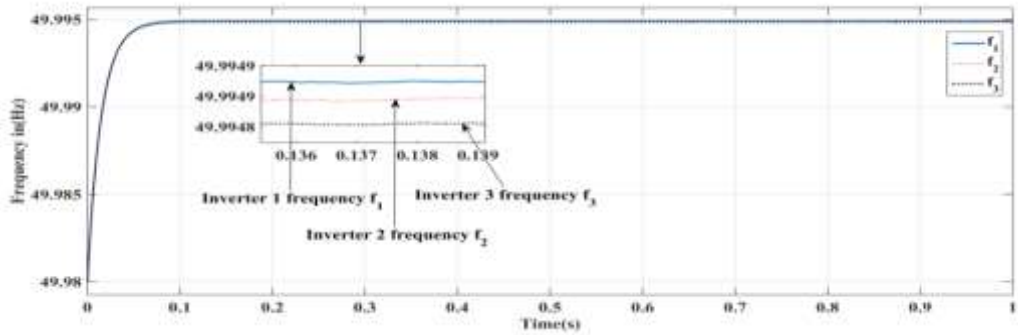


Figure 13. Frequency waveforms of inverters

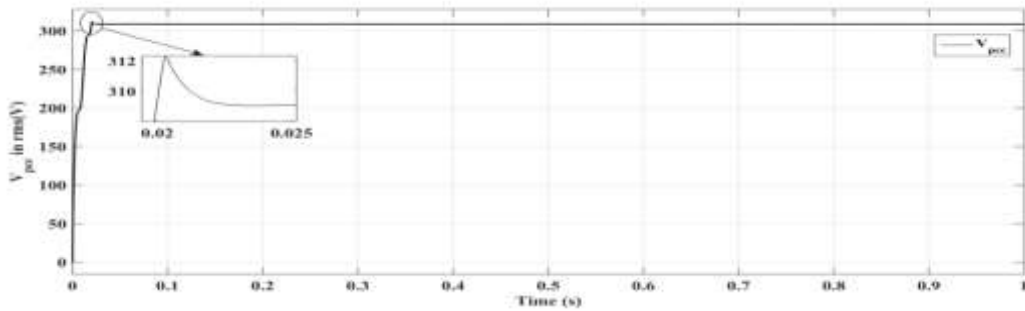


Figure 14. Voltage at PCC(RMS)

3.6.2. Case 2: Power sharing of inverters in microgrid with step changes in the power load

Three inverters are connected in parallel and droop co-efficients and line impedance are taken as $m_1=m_2=m_3=0.0015\text{V/VAR}$, $n_1=n_2=n_3=00001\text{rad/s/W}$ and $R_1=R_2=R_3=0.642\Omega, X_1=X_2=X_3=0.0264\Omega$. Power sharing of each individual inverters is investigated with total load $P_{\text{Load}}=6000\text{W}, Q_{\text{Load}}=16\text{VAR}$. The variation of the load are set at 0.5s. At $t=0$ to 0.5s total load is $P_{\text{Load}1}=4500\text{W}, Q_{\text{Load}1}=10\text{VAR}$ and each inverters is able to share the load proportionally, active power of $P_1=1495\text{W}, P_2=1492\text{W}, P_3=1488\text{W}$ and reactive power of $Q_1=2.6\text{VAR}, Q_2=2.4\text{VAR}, Q_3=2.1\text{VAR}$. At $t=0.5\text{s}$ additional load $P_{\text{Load}2}=1500\text{W}, Q_{\text{Load}2}=6\text{VAR}$ is added in to the microgrid system and each inverters is able to share the load proportionally, $P_1=1989\text{W}, P_2=1983\text{W}, P_3=1977\text{W}$ as shown in the Figure 15 and reactive power of $Q_1=4.3\text{VAR}, Q_2=3.8\text{VAR}, Q_3=3.3\text{VAR}$ as shown in the Figure 16. Frequency variation of inverters is within the range of 49.99Hz to 49.98Hz, the maximum fluctuation of 0.004Hz as shown in the Figure 17. Voltage at PCC can be seen as a slight decline in the voltage amplitude by a 311V to 309V as shown in the Figure 18. Thus, P-V/Q-F droop control ensures that the voltage change is not greater than 5%, the frequency change is not greater than 1% and established a better accuracy and effectiveness in the microgrid system.

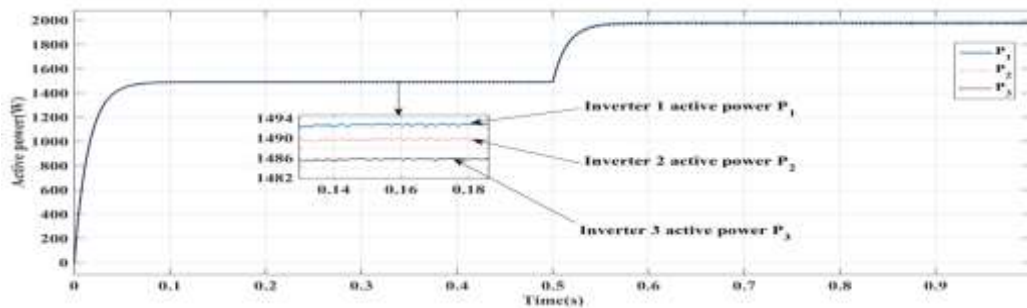


Figure 15. Active power waveforms of inverters with step change load

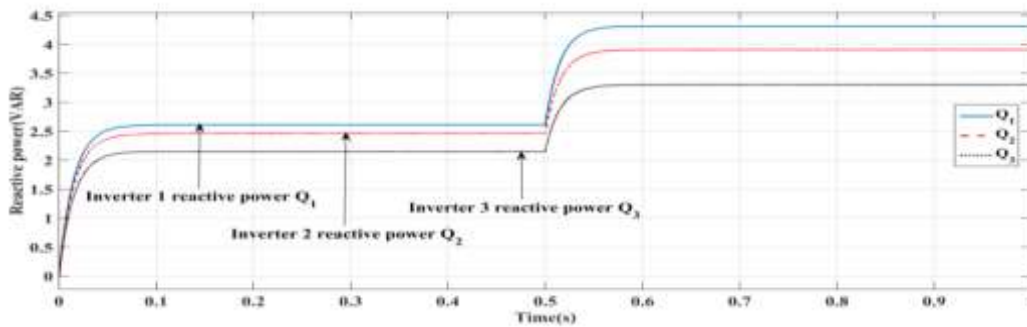


Figure 16. Reactive power waveforms of inverters with step change load

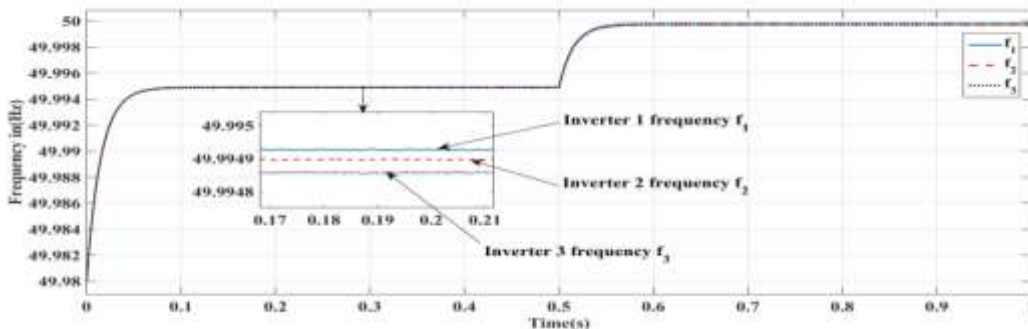


Figure 17. Frequency waveforms of inverters

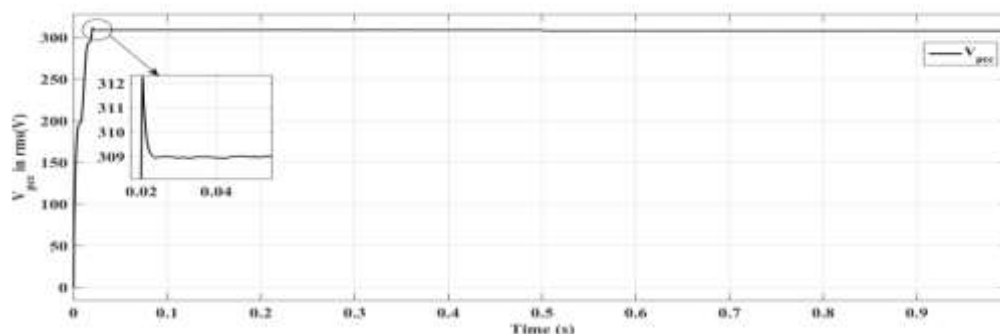


Figure 18. Voltage at PCC(RMS)

4. CONCLUSION

This paper presents a droop control for the stable operation of the inverters in parallel in the absence of interconnection signal line. In order to achieve proportional load sharing among parallel inverters, droop control has been implemented based on voltage and current control strategy. During the load changes microgrid system with droop control quickly responds to suppress voltage and frequency fluctuations. Simulation results show that the droop control strategy can effectively improve the accuracy of load power distribution and has a good dynamic and steady state characteristics.

REFERENCES

- [1] Liserre M, Sauter T, Hung JY, Future energy systems: integrating renewable energy source into the smart power grid through industrial electronics. *IEEE Ind Electron Mag* 4(1):pp:18-37,2010.
- [2] Katiraei F, Iravani MR, Power management strategies for a microgrid with multiple distributed generation units. *IEEE Trans Power Syst* 21(4):pp:1821-1831,2006.
- [3] Carrasco JM, Franquelo LG, Bialasiewicz JT et al, Power electronic systems for the grid integration of renewable energy sources: a survey. *IEEE Trans Power Electron* 19(5):pp:1195-1204,2006.
- [4] Blaabjerg F, Chen Z, Kjaer SB, Power electronics as efficient interface in dispersed power generation systems. *IEEE Trans Power Electron* 19(5):pp:1184-1194,2004.
- [5] Katiraei F, Iravani R, Hatziargyriou N et al, Microgrids management. *IEEE Power Energy Mag* 6(3):54-65,2008.
- [6] Yumei LI, Farzam Nejabatkhah, Overview of control, integration and energy management of microgrids. *J. Mod. Powe Syst. Clean Energy* 2(3):pp:212-222,2014.
- [7] Li YW, Vilathgamuwa DM, Loh PC, Design, analysis, and real-time testing of a controller for multi bus microgrid system. *IEEE Trans Power Electron* 19(5):1195-1204,2004.
- [8] Guerrero JM, Matas J, Luis GDV et al, Wireless- control strategy for parallel operation of distributed-generation inverters. *IEEE Trans on Industrial Electronics* 53(5): pp:1461-1470,2006.
- [9] LIU Wen, A study of master slave control strategy in the isolated microgrid. *Journal of Wuyi university* 25(3):pp:55-59,2011.
- [10] HM Hsieh, TF Wu, HS Nien, A compensation strategy for parallel inverters to achieve precise weighting current distribution. *IEEE IAS Annu Conf. Rec.* pp:954-960,2005.
- [11] M Chandorkar, D Divan, R Aadapa, Control of parallel connected inverters in standalone AC supply systems. *IEEE Trans Ind Appl* 29(1):pp:136-143,1993.
- [12] Guerrero JM, Vasquez JC, Matas J et al, Hierarchical control of droop controlled AC and DC microgrids-A general approach toward standardization. *IEEE Trans Ind Electron* 58(1):pp:158-172,2011.
- [13] W Yao, M Chen, J Matas et al, Design and Analysis of the droop control method for parallel inverters considering the impact of the complex impedance on the power sharing. *IEEE Trans Ind Electron* 58(99):pp:576-588,2010.
- [14] R Majumder, G Ledwich, A Ghosh et al, Droop control of converter interfaced microsources in rural distributed generation. *IEEE Trans Power Del* 25(4):pp:2768-2778,2010.
- [15] JW Kim, HS Choi, BH Cho, A novel droop method for converter parallel operation. *IEEE Trans. Power Electron* 17(1):pp:25-32,2002.
- [16] R Majumder, G Ledwich, A Ghosh et al, Improvement of stability and load sharing in an autonomous microgrid using supplementary droop control loop. *IEEE Trans Power Del* 25(2):pp:796-808,2010.
- [17] Xue Y, Chang L, Kjaer SB et al, Topologies of single phase inverters for small distributed power generators: an overview. *IEEE Trans Power Electron* 19(5):1305-1314,2004.
- [18] Arman Roshan, Rolando Burgos, Andrew C et al, A D-Q frame controller for a full-bridge single phase inverter used in small distributed power generation systems. *IEEE applied power electronics conference* 641-647,2007.
- [19] Loh PC, Holmes DG, Analysis of multiloop control strategies for LC/CL/LCL-filtered voltage source and current source inverters. *IEEE Trans Ind Appl* 41(2):pp:644-654,2005.
- [20] Byoungwoo Ryu, Jaesik Kim, Jaeho Choi et al, Design and analysis of output filter for 3-phase UPS inverter. *IEEE*

power conversion conference 3:941-946,2002.

- [21] Kodanda Ram RBPUSB, Venu Gopala Rao, Operation and control of grid connected hybrid AC/DC microgrid using various RES, *IJPEDS, 5(2):pp:195-202, October 2014.*

BIBLIOGRAPHY OF AUTHORS



Chethan Raj D received his M.Tech from M S Ramaiah institute of technology Bangalore (MSRIT) in the year 2011. Currently he is pursuing his Ph.D. research work in the Department of Electrical and Electronics Engineering at NITK Surathkal. His areas of research interests are Distributed generation, microgrid control and parallel operation of inverters in microgrid.



D N Gaonkar received his Ph.D. from the Indian Institute of technology, Roorkee, India, in 2008. He was a visiting scholar at the University of Saskatchewan Canada, and he is working as an assistant professor in the Department of Electrical and Electronics Engineering, National Institute of Technology Karnataka Surathkal, India. He has published many articles in international journals/conferences and is a senior member of the IEEE. His main research interests are in the areas of power system operation and control, DG, and power electronics.